Non-local electric field effects in magnetized plasmas

IEPC-2005-028

Presented at the 29th International Electric Propulsion Conference, Princeton University, October 31 – November 4, 2005

Cliff A. Thomas*, Nicolas Gascon†, Michelle Allis‡, Emmanuelle Sommier§, and Mark A. Cappelli**
Stanford University, Stanford, CA, 94305-3032

A variety of theories have been proposed to explain electron transport in Hall accelerators, but none is fully compatible with experimental observations. It is proposed and demonstrated that non-local electric field effects on the scale of the electron gyro-radius can impact electron mobility in Hall thrusters. This non-local effect arises as a result of strong E×B shear, due either to fluctuations, or to static field gradients, common to most modern Hall thrusters. Numerical calculations in an r-z hybrid code have recently predicted the existence of strong 2-5MHz axial oscillations characterized by the dispersion relation for a beam-plasma instability. This paper reports the instability, and considering non-local electric field effects, suggests a saturation mechanism for longitudinal electrostatic oscillations in an applied magnetic field. It is found that the instability, as predicted by the numerical simulation, can partially explain the observed transport near the exit plane of the Hall accelerator. The result is expected to apply to many electron-confinement devices using strong magnetic fields, and suggests that E×B shear can be used as a tool for modifying electron mobility in magnetized plasmas.

Nomenclature

$U_{\varsigma m}$	=	velocity of species ς, m direction
n_ς	=	number density of species ς
q_ς	=	charge of species ς
m_ς	=	mass of species ς
R	=	volumetric ionization rate
μ	=	mobility
υ	=	frequency
k	=	wave number
$\boldsymbol{v}$	=	vector velocity
$\boldsymbol{E}$	=	vector electric field
$\boldsymbol{B}$	=	vector magnetic field
c	=	charge per unit mass frequency (q_e/m_e)
Ω_e	=	electron cyclotron frequency (q_eB/m_e)
Ω_e^*	=	apparent electron cyclotron frequency
α	=	**E×B** shear factor
υ_e	=	electron-neutral collision frequency
$\boldsymbol{v}_{en}$	=	drift velocity due to electron-neutral collisions

* Research Assistant, Mechanical Engineering Department. saber@stanford.edu.
† Research Associate, Mechanical Engineering Department. nicolas.gascon@stanford.edu.
‡ Research Assistant, Mechanical Engineering Department. mkallis@stanford.edu.
§ Visiting Researcher, Mechanical Engineering Department. emsom@stanford.edu.
** Professor, Mechanical Engineering Department. cap@stanford.edu.

v_{pd} = polarization drift velocity
S = cyclotron orbit velocity
S^* = effective cyclotron orbit velocity ($S(1-\alpha)^{1/2}$)
γ = angular phase of cyclotron orbit

I. Introduction

In the Hall discharge accelerator[1], or Hall-effect thruster, ion acceleration is achieved between an anode and a hot-emitting cathode by an electrostatic field. Electron motion is impeded by an applied orthogonal magnetic field. Because of their mass, ions are largely unaffected by the magnetic field, and obtain an energy determined by their point of ionization in the potential field. In optimized Hall thrusters, ions ultimately carry 70-90% of the discharge current depending on the effectiveness of the design at inhibiting electron migration. In typical Hall discharges, electrons leak through the magnetic field at a rate unexplained by either classical or Bohm diffusion parameters[1-5]. In many Hall thrusters, the electron mobility is found to vary throughout the channel[3], approaching classical values in some regions, and far exceeding classical values in others (see Fig. 1). This makes the Hall accelerator a challenging device to model for propulsion applications, but also a convenient device for studies pertaining to anomalous electron transport mechanisms.

Many theories have been proposed to explain the anomalous electron mobility in Hall accelerators, but none has been rigorously tested or validated, nor incorporated into a self-consistent simulation that can accurately predict experimental data (such as discharge properties and overall thruster performance). The general problem of conduction across magnetic field lines due to fluctuations in plasma has been investigated theoretically. For example, it has been proposed that anomalous transport can be due to drift wave instabilities that propagate in the **E**×**B** azimuthal direction[6]. These instabilities are thought to create correlated azimuthal electric field and density fluctuations that enhance mobility in the axial direction (along **E**). Another popular theory pertaining specifically to transport in Hall thrusters involves electron-wall interactions[5]. Both fluctuations and wall scattering are possible mechanisms for cross-field electron transport, but neither has evolved to a point where they can adequately explain the body of experimental data now accumulated for Hall thrusters.

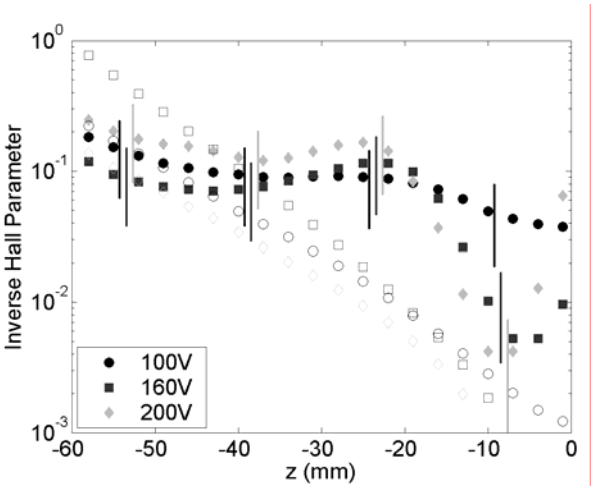

Figure 1. Inverse Hall Parameter in the Stanford SPT[3]. The filled markers are calculated from experimental data, the unfilled markers are classical predictions.

As an alternative theory, it is proposed here that non-local electric field effects on the scale of the electron gyro-radius might impact electron mobility in Hall discharges. Recently, numerical calculations in an r-z hybrid code have predicted the existence of strong 2-5MHz axial fluctuations, the dispersion relation of which is characteristic of a typical ion beam-plasma instability. This paper reports the instability, and considering non-local electric field effects, suggests that longitudinal electrostatic oscillations in an applied magnetic field can account for some of the anomalous transport seen experimentally. We surmise that the growth of this instability is naturally limiting (saturated) by the increasing leakage of electron space charge at large amplitudes.

II. Electron Particle Dynamics

A. The Classical Picture

In the classical picture of electron motion inside the Hall accelerator, electrons are thought to gyrate in well-defined cyclotron orbits while drifting in the **E**×**B** direction. Since the cyclotron frequency is much higher than the electron-neutral collision rate, electrons are thought to drift around the circumference of the Hall accelerator several times before colliding with a neutral atom, scattering randomly, and then re-establishing their cyclotron orbit and **E**×**B** drift. In the presence of an applied electric field, the electron is expected to drift towards the anode with each collision. This drift gives rise to an axial electron current. The classical picture is appealing due to its simplicity, but

over time, the Hall-effect thruster community has come to accept that electron motion and transport in these devices cannot be attributed to a classical description under most circumstances (see Fig. 1).

B. Including Temporal Fluctuations

Attempts have been made to improve the classical picture of transport across magnetic fields by adding temporal fluctuations to the description of electron motion[6], since it is well documented that Hall-effect discharges exhibit strong instabilities[7]. The inclusion of fluctuations through the use of an anomalous Bohm transport mechanism have resulted in some success at describing electron transport in Hall thrusters at low voltage[3], but fail in general to describe discharge properties at high voltages, typical of those where Hall thrusters usually operate (> 150V). It is possible that azimuthal drift wave instabilities may account for enhanced electron transport, but it has been difficult to experimentally ascertain their true extent and magnitude – and whether or not they are solely responsible for the observed electron transport, or merely act in parallel with more important mechanisms.

C. Non-local Electric Field Effects

The consideration of non-local electric field effects is a natural extension of these efforts to identify mechanisms for cross-field transport in Hall thrusters. It is well known that in the acceleration zone of a typical Hall-effect thruster, the plasma potential can vary considerably over a very small spatial scale. Because of this, the mean energy of an electron can vary dramatically over spatial scales comparable to the Larmor radius. It is convenient to introduce a figure of significance, $K = e\phi/(kT)$, which is equal to the change in potential of an electron over its Larmor radius divided by the local electron temperature. A strong change in this value is indicative of regions where non-local effects may become significant. In Fig. 2 above, we plot the spatial variation in K for a laboratory thruster studied extensively at Stanford. For this discharge operating at low voltage (e.g., 100V), the spatial variation in this parameter is subtle. However, at higher discharge voltages, when the acceleration zone is more sharply defined and the **E**×**B** drift velocity is higher, the picture changes dramatically. At 160V and 200V the ratio changes dramatically near the exit plane of the thruster (z = 0). Such an exaggerated variation in particle energy over the local Larmor radius is expected to have a significant effect on particle dynamics and electron mobility. It is hoped that an understanding of these non-local effects can lead to a model for electron mobility that can be used in Hall thruster discharge simulations.

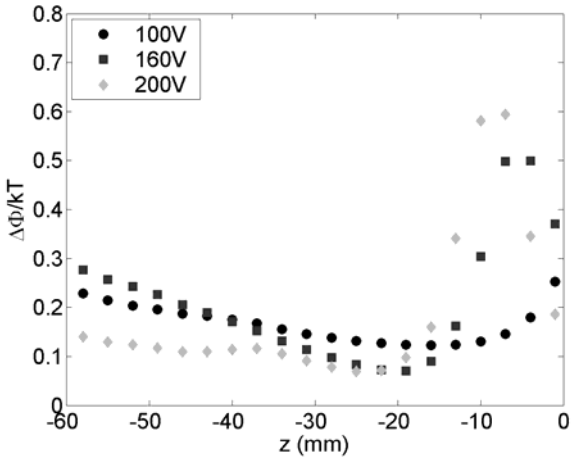

Figure 2. Variation in the plasma potential over the local Larmor radius divided by the local electron temperature in the Stanford SPT.

To understand some non-local effects associated with spatially-varying electric fields, it is useful to start by considering the trajectory of a single electron subject to the Lorentz force in a uniform magnetic field. The electron's charge per unit mass = *c*. The solution to the particle's velocity perpendicular to the magnetic field is given by:

$$\frac{d^2 v_\perp}{dt^2} + \Omega_e^2 v_\perp = c\frac{d\vec{E}}{dt} + c^2 \vec{E}\times\vec{B} \tag{1}$$

Eq. (1) accounts for classical charged particle motion when the electric and magnetic fields are uniform, and **E** is a function of time only. Interesting consequences arise for the case of non-uniform electric fields. The first term on the right side of Eq. (1) can be expanded to account for spatial and temporal variation in **E** to 1st order:

$$\frac{d\vec{E}(\vec{x},t)}{dt} = \nabla_{\vec{x}}\vec{E}\,|_t \cdot v + \frac{d\vec{E}}{dt}|_{\vec{x}} \tag{2}$$

Substituting Eq. (2) into Eq. (1) results in:

$$\frac{d^2 v_\perp}{dt^2} + \left(\Omega_e^2 I - c\nabla_{\vec{x}}\vec{E}\,|_t\right)\cdot v_\perp = c\frac{d\vec{E}}{dt}|_{\vec{x}} + c^2\vec{E}\times\vec{B} \tag{3}$$

Eq. (3) is not dramatically different from Eq. (1) except for in the introduction of an effective cyclotron frequency, and this can be easily represented in the case of an electric field whose gradient is perpendicular to the local magnetic field:

$$\Omega_e^{*2} = \Omega_e{}^2(1-\alpha) \tag{4a}$$

Here, we introduce the electron shear factor:

$$\alpha = \nabla\left(\frac{E\times B}{B^2}\right)\Omega_e{}^{-1} \tag{4b}$$

The electron shear factor is a measure of the characteristic rate at which the **E**×**B** drift velocity varies in comparison to the rate of electron gyration about the local magnetic field.

It is apparent that the effective cyclotron frequency is strongly altered as α approaches 1. However, more interesting is that the effect is asymmetric – i.e., effect of the **E**×**B** shear depends on its sign, and that **E**×**B** shear can increase the apparent cyclotron frequency as easily as it can decrease it[8]. The time-averaged **E**×**B** shear factor, α, is shown for the Stanford discharge in Fig. 3. The maximum estimate of α is +0.15, and α is seen to be large in the region of the thruster where there is a noticeable drop in the inverse Hall parameter (see Fig. 1). As indicated by Eq. 4a, an **E**×**B** shear factor this small would not be expected to change the apparent cyclotron frequency appreciably, and so, it might be concluded that non-local electric field effects do not greatly affect transport. However, this conclusion may rest too strongly on the accuracy of these previous measurements (see below). In addition, as discussed below, local fluctuations in the axial electric field (especially at large wavenumbers) can also introduce non-local field effects. This, together with the effect of a static shear, may account for the transport seen in these devices.

To calculate the electric field gradient in the Stanford thruster, time-averaged measurements of the plasma potential had to be made. These measurements were limited spatially by the averaging over the length scale of the emissive probe that was used (~5mm). The measurements are also post-processed to extract the field through the first derivative[2]. It is expected then that the measured electric field is to be interpreted as a lower limit, and the actual electric field (and its gradient) can be significantly higher than what is published for this discharge. Also, since the **E**×**B** shear factor scales as B^{-2}, even a small uncertainty in the magnetic field can cause a large change in the apparent value of α. Since α in Fig. 3 is computed using vacuum magnetic field data, it does not take into account previous findings that the magnetic field near the exit plane can be reduced by more than 20% at 200V[9] due to the induced Hall current (in comparison to its vacuum value). The conclusion is that the shear factor given in Fig. 3 is necessarily a lower bound, and could be much higher. Support for this conjecture is seen in numerical simulations of the Stanford SPT; simulation values for the time-averaged shear factor exceed those in Fig. 3 by several times[10].

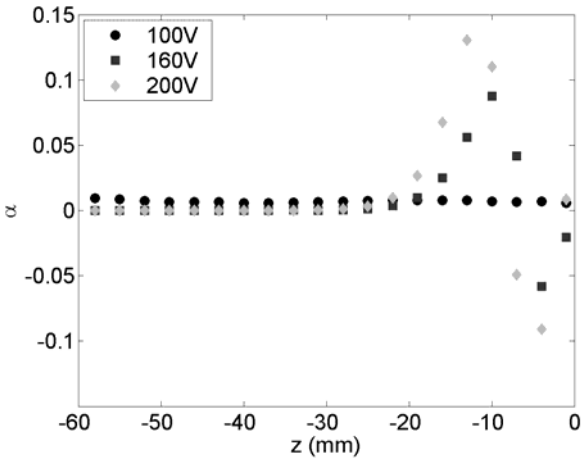

Figure 3. Time-averaged E×B shear factor, α, vs axial position in the Stanford SPT.

With this understanding, no definitive conclusion as to the impact of the static **E**×**B** shear factor on the transport in the Stanford discharge is possible. Despite this, it is likely to have an impact for Hall-effect discharges with steeper potential gradients than that studied here. In fact, the non-local electric field effect detailed above should also affect transport in other magnetized discharges. For example, in the so-called Anodel Layer Thruster (TAL), the ionization and acceleration region is known to be much shorter than that of a typical magnetic layer (SPT) thruster.

Below, we consider the potential impact that fluctuations may have on transport as a result of non-local effects. It is expected that the shear factor due to fluctuations alone will scale as:

$$\alpha = (k_\perp \rho)^2 \left(\frac{e\tilde{\Phi}}{kT} \right) \tag{5}$$

Here, $k_\perp$ is the wave number for a longitudinal electrostatic disturbance, and ρ is the classical Larmor radius. Since it has been shown that $\alpha \propto 1$ marks a regime where the apparent cyclotron frequency is strongly altered (and it seems reasonable that electrostatic disturbances in the Hall accelerator might be comparable to the local temperature), it is expected that axial disturbances with wavelengths comparable to local the Larmor radius could dramatically affect transport. While experiments are presently underway to verify the existence of such fluctuations, numerical experiments carried out with our hybrid thruster simulations have suggested that such fluctuations may exist, due to beam-plasma instabilities.

III. Electrostatic Fluctuations in the Plasma Potential

D. Numerical Experiments

A hybrid particle-in-cell/fluid simulation of a Hall discharge[6] was used to simulate the Stanford discharge. The simulation is based on the hybrid simulation of Fife[7]. It models the ions as discrete particles, advancing them in time according to the local electric field. Electrons are modeled as a fluid with a defined mobility. When an experimentally determined mobility[3] is used, the hybrid simulation does a good job reproducing the experimentally measured electron temperature, electron density, plasma potential, and ion and neutral velocity[10]. This approach was necessary to resolve spatial scales inaccessible to plasma probes.

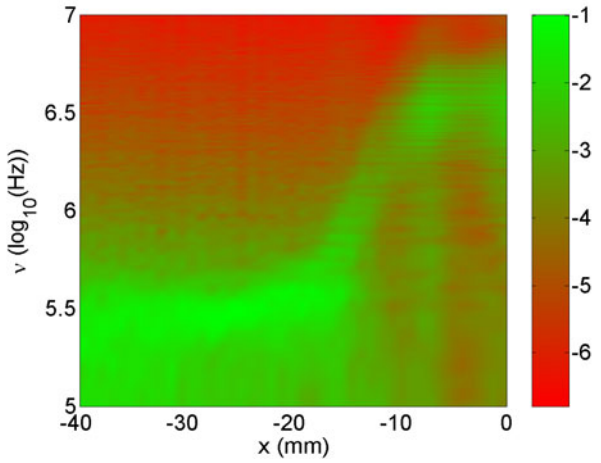

Figure 4. Power spectral density normalized by axial position, in log scale, of the r-z hybrid code's electric field fluctuations at 200V.

An examination of these simulations has revealed the existence of strong 2-5 MHz axial oscillations in the region close to the discharge exit[9] with a wavelength comparable to the local Larmor radius. The variation in the power spectral density of these disturbances is shown in Fig. 4. It is noteworthy that these disturbances are captured when using the experimentally measured mobility, but are not strongly excited when a B^{-1} model is invoked. Historically, MHz level oscillations have been attributed to drift-wave instabilities that propagate in the azimuthal direction[6-7], something this r - z space simulation is incapable of capturing (i.e., it does not model the out of plane or azimuthal direction). It is also noted that MHz level oscillations have been reported in numerous experiments[11-13]. Below, the 2-5MHz instabilities shown in Fig. 4 are analyzed to determine any impact they might have on electron mobility due to non-local electric field effects.

E. Axial Beam Plasma Instability

A preliminary examination of the simulation data suggests the disturbances propagate at speeds close to the ion velocity, and are excited primarily in the region of strong ion acceleration. This finding supports the theory that these fluctuations represent a beam-plasma (streaming) instability with an unresolved azimuthal component. The beam-plasma dispersion relation is obtained using standard perturbation theory applied to a quasi-neutral plasma whose properties vary in the axial direction only, i.e., the direction of the applied electric field**, E**. The one-dimensional mass and momentum conservation equations are given as:

$$\frac{dn_i}{dt} + \frac{d}{dx}\left(n_i U_{i,x}\right) = R \tag{1}$$

$$\frac{dn_e}{dt} + \frac{d}{dx}\left(n_e U_{e,x}\right) = R \tag{2}$$

$$\frac{dU_{i,x}}{dt} + U_{i,x}\frac{dU_{i,x}}{dx} = \frac{q_i}{m_i}E_x - RU_{i,x} \tag{3}$$

$$U_{e,x} = \mu E_x \tag{4}$$

Here, n is the plasma density, $U_{i,x}$ and $U_{e,x}$ are the ion and electron velocity, and m_i and q_i are the ion mass and charge, respectively. R is the net rate of ionization, and μ is the cross-field electron mobility. Most of these properties are prescribed from measurements[2]. The usual perturbations of the sort:

$$\xi = \xi_o(x) + \tilde{\xi}e^{j(kx-wt)} \tag{5}$$

are applied to the governing equations. After linearizing the resulting equation set, the dispersion relation is obtained through the determinant of the matrix of coefficients of the perturbation amplitudes, The resulting dispersion relation is given here as:

$$a_4 k^2 + (a_3 + a_2 j)k + (a_1 + a_0 j) = 0 \tag{6}$$

Here the variables related to physical discharge properties are defined as:

$$a_4 = U_{io}^2 \tag{7a}$$

$$a_3 = -2wU_{io} \tag{7b}$$

$$a_2 = -2U_{io}\frac{dU_{io}}{dx} + \frac{eE_o}{M_i} \tag{7c}$$

$$a_1 = w^2 + R^2 - \left(\frac{dU_{io}}{dx}\right)^2 + \frac{e}{\mu m_i}\left(\frac{dU_{eo}}{dx} - R\right) \tag{7d}$$

$$a_0 = 2w\frac{dU_{io}}{dx} - \frac{ew}{\mu m_i} \tag{7e}$$

It is relatively straightforward to show that in the limit of high frequency, the dispersion relation approaches the expected value for a beam-plasma instability ($w = kU_{io}$), Also, in the analysis leading to the full dispersion relation in Eq. (6), it is implied that the gradient scale length for electron and ion acceleration (~1cm) is larger than the wavelength of the perturbation. The roots of Eq. (6) are obtained numerically. For a 200V discharge in the r-z hybrid code, one finds an unstable solution near the exit plane. Here, it is expected that ion kinetic energy is lost to plasma fluctuations, as seen in the growth of these fluctuations in the r-z simulation. The solution for the dispersion relation of the unstable mode at two axial locations is shown in Figs. 5 and 6. These lines are superimposed onto dispersion maps made from the numerical simulation.

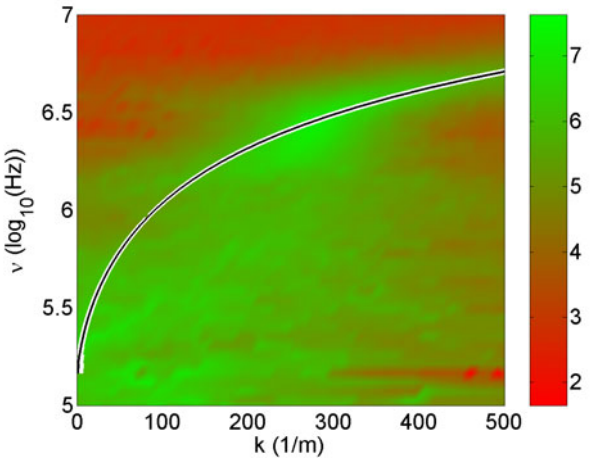

Figure 5. The k-w fluctuation power plotted against the beam-plasma dispersion relation. z = -10mm. U_i = 4700m/s.

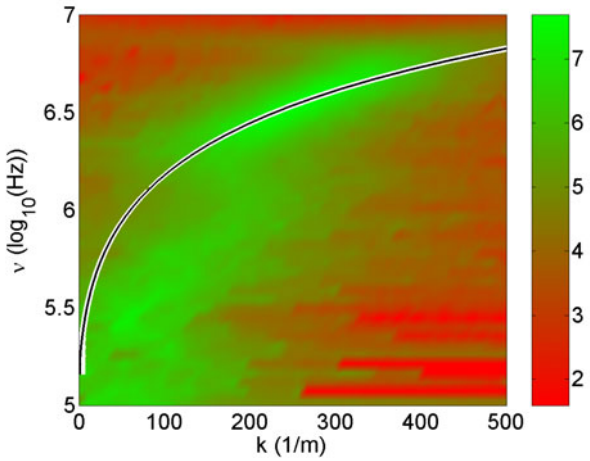

Figure 6. The k-w fluctuation power plotted against the beam-plasma dispersion relation. z = -5mm. U_i = 9500m/s.

The agreement between the dispersion behavior predicted by the analytical model and the simulation support the conjecture that the instability seen in the hybrid simulation is attributable to the beam-plasma instability proposed for 2-5MHz. The limiting solutions also match the values predicted by simulation for wave numbers greater than 200m^{-1}, i.e., the phase velocity of the unstable root is close to the ion velocity. Instabilities with phase velocities of this scale are often referred to as fast "transit time instabilities", and are observed near the exit plane of many Hall accelerators[7,14]. These waves propagate in the direction of ion acceleration. As illustrated above, these instabilities may be more appropriately and broadly described as classical beam-plasma instabilities.

F. Transport due to the Axial Beam-Plasma Instability

To understand how axial instabilities impact electron transport though non-local electric field effects, it is useful to start with Eq. (3). If the fluctuation frequency is much less than the cyclotron frequency, the solution is given by:

$$v_x = \frac{c\dfrac{dE_x}{dt}\Big|_{\vec{x}}}{\Omega_e^{*2}} + \frac{c^2\left(\vec{E}\times\vec{B}\right)_x}{\Omega_e^{*2}} + S\cos(\gamma) \tag{8a}$$

$$v_y = \frac{c\dfrac{dE_y}{dt}\Big|_{\vec{x}}}{\Omega_e^{*2}} + \frac{c^2\left(\vec{E}\times\vec{B}\right)_y}{\Omega_e^{2}} - S^*\sin(\gamma) \tag{8b}$$

For small values of the **E×B** shear factor, we can estimate the cross-field drift due to electron-neutral collisions using the usual expression modified by the effective cyclotron frequency, Ω_e^*, i.e.,

$$v_{en} \cong \frac{\Omega_e \upsilon_e}{\upsilon_e^2 + \Omega_e^{*2}}\left(\frac{E}{B}\right) \tag{9}$$

In a similar fashion, we can determine the impact of a non-uniform electric field through the parameter α to the classical polarization and **E×B** drifts. We consider only the polarization drift due to E_x, as E_y is unresolved in the r-z hybrid simulation. Of course, this is an unfortunate simplification, given that azimuthal instabilities are also expected to impact electron transport. In addition, it is possible the axial instabilities observed in Fig. 4 have an

unresolved azimuthal component. Regardless, interesting behavior can be found considering the axial electric field alone. The polarization drift can be estimated from the first term in Eq. (8a):

$$v_{pd} \cong \frac{1}{\Omega_e(1-\alpha)} \frac{d}{dt}\left(\frac{E}{B}\right) \tag{10}$$

This result is understandable given that Eqs. (8) hold for any particle, and if an isotropic distribution function is assumed in γ, an integration of Eqs. (8) over the distribution function selects only the first two terms of both equations. Eqs. (9) and (10) can be combined to approximate the total cross-field drift due to a strong electric field fluctuation normal to the magnetic field:

$$v_{en} + v_{pd} = \frac{1}{\Omega_e(1-\alpha)}\left(\upsilon_e\left(\frac{E}{B}\right) + \frac{d}{dt}\left(\frac{E}{B}\right)\right) \tag{11}$$

It is apparent that the net drift is substantially modified when α is large and the fluctuation frequency is much greater than the electron-neutral collision rate. As an anecdotal observation regarding the impact of α, it should be considered that for a general electrostatic disturbance, the electric field gradient on either side of the disturbance should reverse sign. Therefore, on one side of the wave a positive shear factor should increase the resultant drift velocity, and on the other side a negative shear factor should reduce it. Since the net drift velocity goes as the inverse of (1-α), the effect is not symmetric. Positive shear factors increase transport more than negative shear factors reduce it – and this causes net transport. Equation (11) can be solved on a time-average basis analytically in the case of small α, for an axially traveling electric field disturbance (see Eq. (12a)).

$$E_x(x,t) = E_o + E_t \sin(kx - wt) \tag{12a}$$

The solution is given by Eq. (12b)

$$\langle v_x \rangle = \frac{\upsilon_e}{\Omega_e}\frac{E}{B} + \left(\frac{\upsilon_e}{\Omega_e}\frac{E}{B} - \frac{w}{k}\right)\sum_{n=2,4,6}^{\infty} \frac{(n-1)!!}{(n)!!}(\max(\alpha))^n \tag{12b}$$

In Eq. (12b), max(α) refers to the maximum **E×B** shear factor of a wave. It is theorized that as the fluctuation intensity of an unstable mode grows, such as the axial beam-plasma instability reported in this paper, the impact of the non-local electric field grows. Of course, the small **E×B** shear factor approximation becomes less accurate. Regardless, it is surmised that as the mobility-coupled beam-plasma instability grows, and as its intensity approaches a level where max(α)=1, the nonlinear response increases. There is a concomitant increase in electron mobility in this situation, which will then feed back to limit growth; i.e., the wave is expected to saturate. In the linear model described above, the mobility is taken to be a constant. Future studies will expand this model into a non-linear regime, to better understand the details of this saturation process.

IV. Potential Impact on Transport in the Laboratory Thruster

F. The Stanford Thruster

To better understand the potential impact of the observed beam-plasma instability on transport in our experimental discharge, the electron-fluid momentum equation is solved using an implicit code in the presence of electric field disturbances defined in space and time with various frequencies and wavenumbers (see Eq. (12a)). The implicit code is second-order accurate in space and time, and includes the electron momentum equation's full material derivative. This is necessary in order to capture the non-linearities imposed by non-local electric field effects. To approximate conditions similar to those near the exit plane of a Hall accelerator and to emphasize the importance of α on anomalous transport, the electron-neutral collision rate is set equal to the minimum value measured for the Stanford thruster at 200V. The resulting classical Hall parameter is 1000 (see Fig. 1). To approximate the intensity of fluctuations seen the hybrid simulation without directly porting the simulation's electric field history (since this electric field history is defined by a comparably rough grid in space and time), an average

electric field of 2000V/m is assumed for the implicit code, and the fluctuation amplitude of the electric field is set equal to this value. Both values are representative of observed values, but it should be noted that the fluctuations in the hybrid simulation necessarily represent a more broadband spectrum than any single disturbance as defined in Eq. 12a. The proper resolution of this spectrum is expected to increase electron transport compared to a simple calculation at one frequency. Also, the choice of a 2000V/m fluctuation is conservative, and this value could reasonably be changed to a value two times higher. If this were so, the resulting anomalous transport would be much greater (since the effect we are considering is strongly nonlinear). These choices are made so that the resulting computation is easily understood, and can be considered to place a lower bound on the potential impact of the axial disturbances reported in Fig. 4. The solution is shown in Fig. 7.

In Fig. 7, it is readily apparent the effective time-average Hall parameter is substantially altered for axial disturbances at 2-5MHz for wavelengths comparable to the local Larmor radius. If one considers the dispersion maps for the hybrid simulation, Figs. 5 and 6, it is reasonable to conclude that the observed axial fluctuations can reduce the Hall parameter near the exit plane to less than 200 (given that Fig. 7 is a conservative estimate). From the results shown in Fig. 1, it is seen that axial fluctuations of the type reported in Section **III** can explain the anomalous transport near the exit plane of the Hall accelerator. Given any finding that the disturbances detailed in Figs. 5 and 6 extend to even higher frequencies and smaller wavenumbers, or are more intense than the values found in the hybrid numerical simulation, this conclusion would be even more certain.

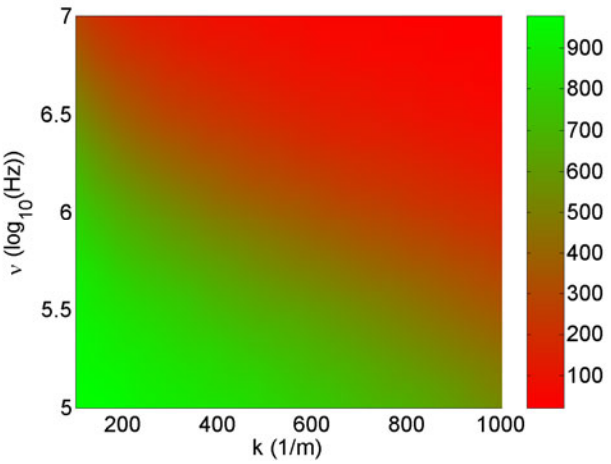

Figure 7. The <HP> calculated from the electron momentum equation due to a traveling electric field disturbance. E_t = 2000V/m. E_o = 2000V/m. B=0.01T.

An electron PIC code was developed to determine the accuracy of the results for Fig. 7. The PIC code was developed for the expressed purpose of analyzing non-local electric fields on particle dynamics with high fidelity. The code is implicit, and second order in space and time. The code's time step is chosen to accurately resolve the classical cyclotron frequency, and the spatial grid is made to resolve the Larmor radius. This check was thought to be necessary given that a fluid description could become inaccurate for high **E×B** shear, as the electron distribution function might become anisotropic under this condition. As it was, the results were found to mirror the results of Fig. 7 except for the highest values of α considered. At shear factors approaching unity both solutions would saturate, but at slightly different values of the Hall parameter. Despite this, the saturation Hall parameter was comparable to 16 for both (the Bohm value).

As a final note regarding the connection between the observed axial disturbances, non-local electric field effects, and the resulting anomalous transport in the Stanford thruster, it should be remembered that the time-average electric field gradient at different locations in the discharge is finite under most circumstances (see Fig. 3). For the calculation in Fig. 7, the time-average electric field is assumed to be uniform in space. Including the time-average electric field gradient should impact this calculation, since disturbances in the electric field are considered to be superimposed onto a background static value. If this is the case, in the section of the acceleration zone where the electric field gradient points out of the Hall accelerator, the effect of an axial disturbance on transport should be diminished compared to Fig. 7. This is the case since it will take a larger disturbance to cause a high positive shear factor. Near the exit plane of the Hall-effect thruster however, where the time-average electric field gradient points towards the anode, the static electric field gradient will increase transport for any given disturbance, since their positive shear factors will be cumulative. The net understanding is that in the region of the Hall-effect thruster where acceleration first begins to occur and the resulting beam-plasma disturbance is small, the transport will likely be governed by classical collisions and other mechanisms. As the disturbance grows however, towards the exit plane of the Hall accelerator the beam-plasma instability will increase electron transport. To improve upon this model, the beam-plasma instability must be coupled to the resulting mobility.

V. Conclusions and Future Work

Evidence is found to suggest that non-local electric field effects on the scale of the electron gyro-radius could have a significant impact on the electron mobility in the Hall accelerator. Numerical calculations in an r-z hybrid code predict strong 2-5MHz axial oscillations characterized by the dispersion relation for a beam-plasma instability – these oscillations are only apparent when the hybrid simulation relies on the experimentally measured electron mobility, and it is uncertain whether these instabilities have an azimuthal component that is not considered in the simulation. When non-local electric field effects are considered, the saturation of the observed instability is found to be a possible explanation for electron transport near the exit plane of the Hall accelerator. Future work will couple the beam-plasma instability and the mobility, take the full electric field profile of the Hall accelerator into account in the analysis, and examine the Stanford thruster for 1-10MHz axial fluctuations using a high frequency plasma probe. Theory suggests the time-average electric field profile and the overlying disturbances must be considered in tandem to result at the correct conclusion regarding non-local electric field effects on the electron mobility. The time-average **E×B** shear appears to effect transport in the Hall accelerator, and theory suggests it may be a tool for modifying electron mobility in magnetized plasmas.

Both fluid and PIC simulations are found to reveal a saturation in anomalous transport due to axial disturbances at a Hall parameter comparable to the Bohm value. This suggests that for fluctuations in the potential comparable to the local electron temperature, the interaction of electrons with their self-induced potential fluctuations is strong, and results in momentum scattering at a rate comparable to the cyclotron frequency. This is sufficient to explain the saturation Hall parameter of ~16, and perhaps B^{-1} transport in general (due to longitudinal disturbances).

VI. Acknowledgements

This research was supported by the Air Force Office of Scientific Research. C. A. Thomas also received support from the National Science Foundation, and from Stanford University through the Stanford University Graduate Fellowship Program.

VII. References

[1]G.S. Lanes and R.S. Lowder, *Physics of Fluids*, 9, 1115 (1966).
[2]N.B. Meezan, W.A. Hargus, and M.A. Cappelli, *Physical Review E*, 63, 026420. (2001).
[3]N.B. Meezan, and M.A. Cappelli, *Physical Review E*, 66, 036401 (2002).
[4]J. Fife, and M. Martinez-Sanchez, AIAA-96-3197 (1996).
[5]A.I. Morozov, and V.V. Savelyev, *Reviews of Plasma Physics*, 21, 203. (2000).
[6]S. Yoshikawa, and D.J. Rose, *Physics of Fluids*, 5, 334 (1962).
[7]E.Y. Choueiri. AIAA-94-3013 (1994).
[8]K.C. Shaing, A.Y. Aydemir, and R.D. Hazeltine, *Physics of Plasmas*, 5(10) (1998).
[9]C.A. Thomas, and M.A. Cappelli, AIAA-05-4063 (2005).
[10]M.K. Allis, N. Gascon, C. Vialard-Goudou, M.A. Cappelli, E. Fernandez., AIAA-04-3951 (2004).
[11]C.A. Thomas, N. Gascon, and M.A. Cappelli. AIAA-03-4854 (2005).
[12]N.B, Meezan, W.A. Hargus, and M.A. Cappelli, AIAA-1998-3502 (1998).
[13]A. Lazurenko, V. Vial, M. Prioul, and A. Bouchoule, *Physics of Plasmas*, 12, 013501. (2005).
[14]S. Barral, K. Makowski, Z. Peradzynski, and M. Dudeck, *Physics of Plasmas*, 12, 073504 (2005).